

**K-shell ionization by antiprotons**

G. Mehler, B. Müller, and W. Greiner

*Institut für Theoretische Physik der Universität Frankfurt, Robert-Mayer-Strasse 8-10, D-6000 Frankfurt, West Germany*

G. Soff

*Gesellschaft für Schwerionenforschung, Planckstrasse 1, Postfach 11 05 41, D-6100 Darmstadt, West Germany*

(Received 13 January 1987)

We present calculations for the impact-parameter dependence of *K*-shell ionization rates in  $\bar{p}$ -Cu and in  $\bar{p}$ -Ag collisions at various projectile energies. We show that the effect of the attractive Coulomb potential on the Rutherford trajectory and the antibinding effect caused by the negative charge of the antiproton result in a considerable increase of the ionization probability. Total ionization cross sections for proton and antiproton projectiles are compared with each other and with experimental ionization cross sections for protons.

Recently, first measurements of atomic ionization cross sections by antiprotons have been performed by Andersen *et al.*<sup>1</sup> at the CERN low-energy antiproton ring (LEAR). The use of antiprotons in atomic scattering processes is a valuable tool that provides additional insight into the mechanisms of inner-shell ionization which otherwise cannot easily be derived from experiments with ordinary projectiles. In particular, our understanding of the binding effect, which, loosely speaking, reverses sign and becomes an antibinding effect, can be directly tested by a comparison of ionization rates due to protons and antiprotons. A second difference, which distinguishes *K*-shell ionization by antiprotons from *K*-shell ionization by protons, is due to the change in the Rutherford trajectory caused by the replacement of the repulsive nuclear Coulomb potential by an attractive potential.

The enhancement of *K*-shell ionization due to a Rutherford trajectory within an attractive potential has already been predicted by Amundsen.<sup>2</sup> His calculation is based on the semiclassical approach (SCA), taking into account for the description of the projectile potential only its monopole term. Martir *et al.*<sup>3</sup> presented theoretical ratios of cross sections within a coupled-channel approach based on Hartree-Fock wave functions and pseudostates for the description of the electron continuum. Within the framework of the perturbed-stationary-state approach, Basbas *et al.*<sup>4</sup> discussed also ratios of total cross sections for proton and antiproton projectiles. Both calculations demonstrated the enhancement of *K*-shell ionization cross sections due to the antibinding effect and the modified Rutherford trajectory. There is a comparison of impact-parameter-dependent ionization probabilities, for proton and antiproton on Cu at a kinetic energy of 0.5 MeV by Trautmann *et al.*<sup>5</sup> They have made use of wave functions similar to those of this paper within the framework of the SCA method. We will refer to these calculations later on. In the following we present a quantitative analysis of the antibinding effect and the influence of projectile motion within a coupled-channel approach based on relativistic Dirac-Fock-Slater wave functions and the description of the electron continuum by means of relativistic wave

packets.<sup>6,7</sup> At the beam energies available at LEAR (1–10 MeV), ionization by (anti)proton impact may be described in the semiclassical approximation.<sup>8</sup> The nuclear trajectory is specified by classical motion in the Coulomb potential between the (anti)proton and the target nucleus; screening effects on the trajectory may be neglected. For inner-shell ionization of heavy target atoms the use of independent-electron wave functions in a screened potential is appropriate.<sup>9</sup> We then can make use of the theoretical methods described in Refs. 6 and 7. We solve the time-dependent Dirac equation by expanding the wave function of the electron into a basis of atomic Dirac wave functions of the target. This expansion leads to the representation of the Dirac equation as a system of first-order coupled differential equations, which may be solved numerically after suitable truncation:

$$\frac{d}{dt} a_{sf}(t) = -i \sum_k a_{sk}(t) \left\langle \phi_f(\mathbf{r}) \left| \frac{\mp Z_P e^2}{|\mathbf{r} - \mathbf{R}(t)|} \right| \phi_k(\mathbf{r}) \right\rangle \times \exp[i(E_f - E_k)t]. \quad (1)$$

The  $a_{sf}$  denote the time-dependent occupation amplitudes of an atomic state  $f$  by the electron initially occupying the state  $s$ . In the calculations presented below the index  $s$  indicates one of the two *K*-shell electrons. The summation over  $k$  is understood to include discrete as well as continuum states. The basis states  $\phi_k(\mathbf{r})e^{-iE_k t}$  are taken as eigenstates of the Dirac Hamiltonian of the target atom, which includes an effective electron-electron potential in the Dirac-Fock-Slater approximation. We note that, since the formalism is based on the independent-particle picture, explicit electron-electron correlations are neglected, vitiating application to few-electron systems such as helium. By expanding the time-dependent projectile potential [the minus sign in Eq. (1) pertains to protons, the plus sign to antiprotons] into a series of multipoles, the interaction between different states is decomposed into a sum of multipole contributions. As has been shown earlier,<sup>6,9</sup> the multipole expansion converges very fast and can be trun-

cated after the dipole term for the systems of interest here. The numerical integration over the continuous spectrum in Eq. (1) requires a discretization of the electron continuum. This is achieved by integrating the continuum solutions of the atomic Dirac equation within an appropriately chosen energy interval  $\Delta E$ , thus generating relativistic wave packets for the emitted electrons.

As has been mentioned above, our method is not suited to account for the experiment of Andersen *et al.*<sup>1</sup> In  $p$ -He collisions the correlations between the two electrons play a decisive role for the ratio of single to double ionization<sup>10</sup> and the same holds true for  $\bar{p}$ -He collisions. These correlation effects cannot be reproduced by our method because it neglects explicit electron correlations. Furthermore, the semiclassical approximation is not valid in these  $\bar{p}$ -He collisions because the Bohr-Sommerfeld parameter  $\eta$  is in the range  $\eta < 1$ . Recently, Reading *et al.*<sup>11</sup> have presented calculations for the ratio of single to double ionization of helium by protons and antiprotons as measured by Andersen *et al.* They have reproduced the absolute values of the experiment within deviations of about 35% using the forced-impulse method.

However, in collision systems involving targets with higher nuclear charge ( $Z_T > 20$ ), the problems mentioned above do not exist. We have chosen to demonstrate the different effects of  $K$ -shell ionization by protons and antiprotons in the  $^{29}\text{Cu}$  and the  $^{47}\text{Ag}$  target systems, for which there is a large collection of proton ionization data available. Paul and Muhr<sup>12</sup> have combined various experimental data on total  $K$ -shell ionization cross sections into a set of reference ionization cross sections for protons on different target systems, among them Cu and Ag. These values will be used as a check for our results for  $p$ -Cu and  $p$ -Ag collisions and as a comparison for the corresponding results obtained for  $\bar{p}$ -Cu and  $\bar{p}$ -Ag collisions.

In Fig. 1(a) and 1(b) we present our results for the ionization rates in  $p$  and  $\bar{p}$  impact on Cu and Ag, respective-

ly, as function of impact parameter. The results are shown for four different projectile energies ranging from 0.2 MeV up to 5 MeV. The solid lines represent the antiproton results, whereas the proton results are rendered by dashed lines. About 40 bound states and 80 continuum states have been included in the coupled-channel equations for the amplitudes  $a_{sf}$ . The steep rise of the ionization probability at small impact parameters ( $b \leq 50$  fm) is due to the dipole term of the projectile potential. The small oscillating structures, which arise in the  $\bar{p}$  collisions at low energies, are a consequence of the different angular dependence of the dipole term along the classical trajectory in an attractive potential. Our result in the  $\bar{p}$ -Cu System at 0.5-MeV kinetic energy agrees with the result published by Trautmann.<sup>5</sup> However, for the proton projectile our calculations yield ionization rates, which are about a factor 0.5 below the results of Trautmann *et al.* The comparison with experimental cross sections as well as with impact-parameter-dependent probabilities<sup>13</sup> supports our results. Note that the calculations do not take the recoil motion of the target into account but its effects are expected to be negligible except in almost central collisions.<sup>14</sup> The use of antiprotons as projectiles enhances the ionization probability at low projectile energies by roughly an order of magnitude compared to proton collisions. The enhancement factor decreases with higher projectile energy.

This effect is further illustrated in Fig. 2 which presents our results for the total ionization cross section displayed versus the scaled projectile velocity  $\xi = 2v_p/\theta_K v_{TK}$  where  $v_p$  denotes the velocity of the projectile and  $v_{TK}$  the Bohr velocity of the target  $K$ -shell electron. The parameter  $\theta_K$  is given by  $I_K/(Z_T^2 \mathcal{R})$  with  $\mathcal{R} = 13.6$  eV and  $I_K$  is the binding energy resulting from Dirac-Fock-Slater calculations. Again, the solid lines represent the results for antiprotons and the dashed lines those for proton projectiles. The data points represent the reference cross sections of

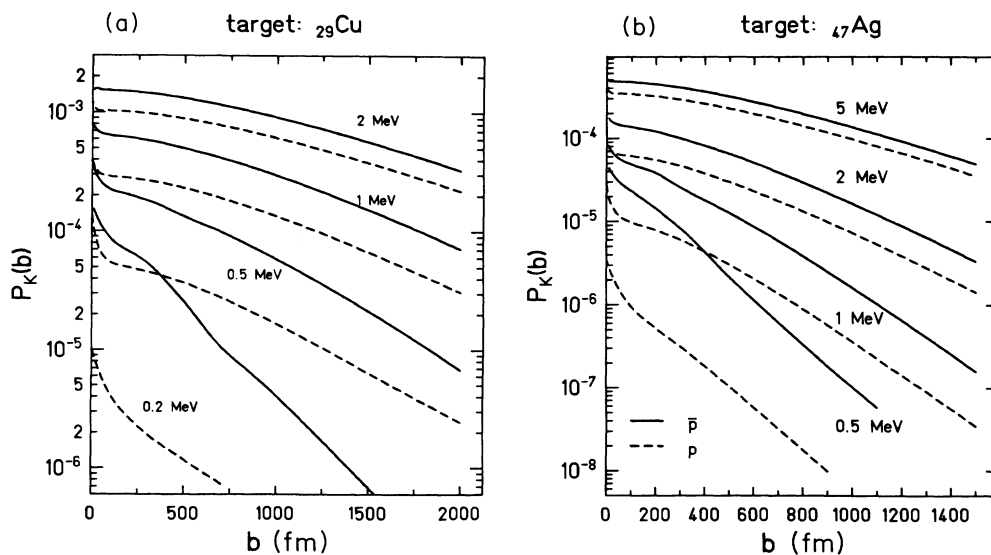


FIG. 1. (a) The  $K$ -shell ionization rates in dependence of the impact parameter  $b$  at four projectile energies for the collision systems  $p$ -Cu (dashed lines) and  $\bar{p}$ -Cu (solid lines) are shown. (b) The same as 1(a) for the Ag target.

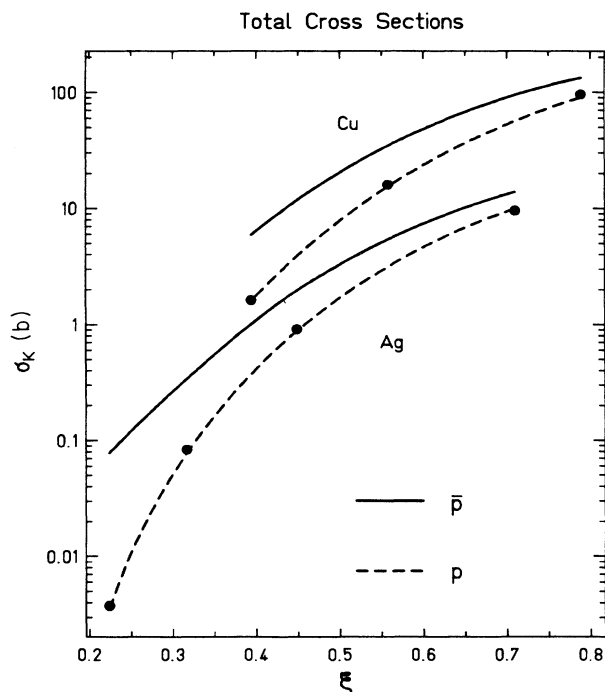


FIG. 2. The total  $K$ -shell ionization cross sections (in barn) for the projectiles  $p$  (dashed lines) and  $\bar{p}$  (solid lines) on Cu and on Ag are shown vs the scaled velocity  $\xi$ . The points represent the experimental reference cross section as given by Paul *et al.* (Ref. 12).

Paul *et al.*<sup>12</sup> Our calculated results for protons are within the error given by Paul, except for the  $p$ -on-Cu data at 2-MeV projectile energy, where our result deviates by about 7% from the reference cross section. Note that the lowest value of  $\xi$  for the Cu target corresponds to a kinetic energy of 0.5 MeV of the projectile. Due to numerical difficulties we do not show the total cross section at a projectile energy of 0.2 MeV.

We now turn to a quantitative discussion of the effects of antibinding and of projectile motion in an attractive potential expressed by these results. To this end we have performed calculations using first-order perturbation theory without further corrections and including only the monopole contribution of the projectile potential. The results of these calculations are depicted in Fig. 3 for  $p$  and  $\bar{p}$  collisions on Ag at an energy  $E_{\text{kin}}=1$  MeV. The two central curves 1 and 2 display ionization rates obtained in first-order perturbation theory for proton (solid line) and antiproton (dashed line) projectiles, respectively. The enhancement of the ionization for antiproton projectiles is solely due to the different trajectory. As we considered only monopole contributions, it results from the different time dependence of the distance between projectile and target  $R(t)$ , whereas the different angular dependence does not influence the results in this approximation. The reason for the enhancement is twofold: First, the antiproton approaches nearer to the target by  $2d\epsilon$ ,  $\epsilon$  being the eccentricity of the Rutherford hyperbola and  $d$  being the collision diameter  $d = Z_p Z_T e^2 / 2E_p$ . Second, the antipro-

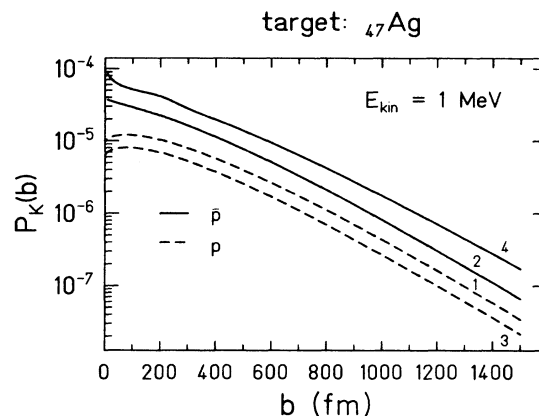


FIG. 3. The results for the differential  $K$ -shell ionization probability vs impact parameter are shown using only the monopole contribution of the projectile potential for antiproton (solid lines) and proton (dashed lines) projectiles on Ag at a kinetic energy of 1 MeV. Curves 1 and 2 represent the results of a first-order calculation, whereas curves 3 and 4 contain the influence of the diagonal matrix element of the  $1s$ -bound state, reproducing the binding and antibinding effects for proton and antiproton, respectively.

ton is accelerated in the vicinity of the target, whereas the proton is slowed down causing a decline of the ionization rate at small impact parameters. This tendency is not seen for antiprotons. In the approximation discussed above the ratio of the proton and antiproton ionization rate has already been given by Amundsen:<sup>2</sup>

$$\frac{dI^-/dE_f}{dI^+/dE_f} \approx e^{2\pi qd}, \quad (2)$$

where  $q = (E_f - E_i) / \hbar v_p$  is the minimum momentum transfer to the electron. Here  $dI^\pm/dE_f$  are the differential ionization probabilities per final electron energy  $E_f$  for antiprotons and protons, respectively. Note that this ratio does not depend on the impact parameter. In the example shown in Fig. 3, the expression (2) amounts to a factor of about 2, in good agreement with the numerical result.

The two outer curves of Fig. 3, curves 3 and 4, result from taking into account the diagonal matrix element of the projectile potential with the  $1s$ -bound state in Eq. (1). The diagonal element accounts for the change in the binding energy of the  $K$ -shell electrons due to the presence of the projectile charge at a distance  $R(t)$ . By comparing the various curves in Fig. 3 we find that the antibinding for antiprotons affects the ionization probability in a varying degree depending on the impact parameter. At an impact parameter of  $b=500$  fm the ionization is raised by roughly 80% and at  $b=1500$  fm by about 160%. By contrast, the binding effect for protons is almost independent of the impact parameter reducing the ionization probability by about 40%. Combined with the trajectory effect, we find that in this approximation the ionization rate is higher by a factor of about 6 for antiprotons as compared with protons at a bombarding energy of 1 MeV. The bombarding-energy dependence exhibited by the re-

sults shown in Figs. 1 and 2 is also readily understood from formula (2). The collision diameter  $d$  becomes smaller with growing projectile energy and thus the ratio of particle to antiparticle ionization declines. As has been pointed out by Basbas *et al.*,<sup>15</sup> the binding is also velocity dependent and vanishes with increasing projectile energy. The same holds true for the antibinding effect. Our calculations show that at 5-MeV projectile energy in the  $p$ -Ag system, the binding effect reduces the ionization by about 20%. At the same projectile energy the antibinding yields

an enhancement in the same order of magnitude.

In conclusion, we have presented quantitative predictions for  $K$ -shell ionization of heavy atoms by antiprotons, including trajectory and antibinding effects. Measurements of  $K$ -shell ionization cross sections with antiprotons and comparison with proton data would allow for a clear experimental separation of the influence of these effects.

We wish to thank J. Reinhardt for carefully reading our manuscript and valuable suggestions.

- 
- <sup>1</sup>L. H. Andersen, P. Hvelplund, H. Knudsen, and S. P. Møller, *Phys. Rev. Lett.* **57**, 2147 (1986).  
<sup>2</sup>P. A. Amundsen, *J. Phys. B* **10**, 2177 (1977).  
<sup>3</sup>M. H. Martir, A. L. Ford, J. F. Reading, and R. L. Becker, *J. Phys. B* **15**, 1729 (1982).  
<sup>4</sup>G. Basbas and W. Brandt, *Phys. Rev. A* **27**, 578 (1983); **28**, 3142(E) (1983).  
<sup>5</sup>D. Trautmann, F. Rösel, and G. Baur, *Nucl. Instrum. Methods* **214**, 21 (1983).  
<sup>6</sup>G. Mehler, G. Soff, T. de Reus, U. Müller, J. Reinhardt, B. Müller, and W. Greiner, *Nucl. Instrum. Methods A* **240**, 559 (1985).  
<sup>7</sup>G. Mehler, G. Soff, and W. Greiner, *J. Phys. B* (to be published).

- <sup>8</sup>J. Bang and J. M. Hansteen, *K. Dan. Vidensk. Selsk. Mat. Fys. Medd.* **31**, No. 13 (1959).  
<sup>9</sup>M. Pauli, F. Rösel, and D. Trautmann, *J. Phys. B* **11**, 2511 (1978).  
<sup>10</sup>A. L. Ford and J. F. Reading, *Nucl. Instrum. Methods B* **10/11**, 12 (1985).  
<sup>11</sup>J. F. Reading and A. L. Ford, *Phys. Rev. Lett.* **58**, 543 (1987).  
<sup>12</sup>H. Paul and J. Muhr, *Phys. Rep.* **135** (1986).  
<sup>13</sup>J. U. Andersen, E. Lægsgaard, and M. Lund, *Nucl. Instrum. Methods* **192**, 79 (1982).  
<sup>14</sup>F. Rösel, D. Trautmann, and G. Baur, *Nucl. Instrum. Methods* **192**, 13 (1982).  
<sup>15</sup>G. Basbas, W. Brandt, and R. Laubert, *Phys. Rev. A* **7**, 982 (1973).